JHEP

Published for SISSA by Springer

Received: August 30, 2018
Revised: October 26, 2018
Accepted: January 5, 2019
Published: January 9, 2019

Same-sign multilepton signatures of an $SU(2)_R$ quintuplet at the LHC

Sanjib Kumar Agarwalla,[a,b] **Kirtiman Ghosh,**[a,b] **Nilanjana Kumar**[c] **and Ayon Patra**[d]

[a] *Institute of Physics, Sachivalaya Marg, Sainik School Post, Bhubaneswar 751005, India*
[b] *Homi Bhabha National Institute, Training School Complex, Anushakti Nagar, Mumbai 400085, India*
[c] *Saha Institute of Nuclear Physics, HBNI, 1/AF Bidhan Nagar, Kolkata 700064, India*
[d] *Centre for High Energy Physics, Indian Institute of Science, Bangalore 560012, India*

E-mail: sanjib@iopb.res.in, kirtiman.ghosh@iopb.res.in, nilanjana.kumar@saha.ac.in, ayon@okstate.edu

Abstract: We study in detail the collider signatures of an $SU(2)_R$ fermionic quintuplet in the framework of left-right symmetric model in the context of the 13 TeV LHC. Apart from giving a viable dark matter candidate (χ^0), this model provides unique collider imprints in the form of same-sign multileptons through the decays of multi-charged components of the quintuplet. In particular, we consider the scenario where the quintuplet carries $(B-L) = 4$ charge, allowing for the presence of high charge-multiplicity particles with relatively larger mass differences among them compared to $(B-L) = 0$ or 2. In this paper, we mainly focus on the same-sign n-lepton signatures (nSSL). We show that with an integrated luminosity of 500 fb^{-1}, the mass of the neutral component, $M_{\chi^0} \leq 480$ (800) GeV can be excluded at 95% CL in the 2SSL (3SSL) channel after imposing several selection criteria. We also show that a 5σ discovery is also achievable if $M_{\chi^0} \leq 390$ (750) GeV in the 2SSL (3SSL) channel with 1000 fb^{-1} integrated luminosity.

Keywords: Beyond Standard Model, Higgs Physics

ArXiv ePrint: 1808.02904

https://doi.org/10.1007/JHEP01(2019)080

JHEP01(2019)080

Contents

1 Introduction

The Standard model (SM) of particle physics is the most successful description of the fundamental particles and interactions. Almost all the predictions of the SM have been verified by different experiments. Yet a number of terrestrial and extra-terrestrial observations compel us to think of the SM as a low energy theory requiring new physics at the high scale. The observation of neutrino oscillation, existence of dark matter (DM) and dark energy, baryon asymmetry of the universe are a few among the many anomalies that have been observed so far. Some of these anomalies, including the generation of light neutrino masses and the existence of a suitable DM candidate can be addressed in the Quintuplet Dark Matter model [1–3] in a left-right (LR) symmetric framework that has been considered in the present work. This model is inspired by Minimal Dark Matter [4–7] scenario and can also give rise to very interesting collider signatures, which we have studied in detail in this paper.

Minimal Dark Matter models are minimal extensions of the SM with a bosonic or fermionic multiplet which include a stable (over the lifetime of the universe), colored and electrically neutral particle candidate for DM. These new multiplets are chosen to be an n-tuplet of the SU(2) group with no strong interactions. The stability of the n-tuplet is either accidental or is ensured by some discrete symmetry. A quintuplet fermionic multiplet is unique in the sense that it is the smallest multiplet which does not require any discrete symmetries to ascertain the stability of its neutral component. For example, the SM fermions and scalars being doublets or singlets under SU(2), the neutral component of a SU(2) quintuplet fermion can only decay into SM particles through operators with mass dimension 6 or higher. Thus its decay width is suppressed at least by a factor of $1/\Lambda^2$, where Λ is the scale of new physics. In this scenario, one can ensure the stability of a

JHEP01(2019)080

TeV scale DM for $\Lambda \gtrsim 10^{14}$ GeV. An $SU(2)_L$ quintuplet on the other hand has severe constraints from observed DM relic density and limits on DM-nucleon scattering cross-section from direct DM detection experiments. Also, due to small radiative corrections from the SM gauge bosons ($W^{\pm}$, Z and photon), the particles in an $SU(2)_L$ quintuplet are nearly degenerate (only a few hundred MeV splitting). Therefore, the decay of a component of the quintuplet to another component gives rise to soft leptons/jets making it difficult to detect at the collider experiments. However, one can exploit these small mass splittings to search for the $SU(2)_L$ quintuplet fermion particles using disappearing track signature [8]. $SU(2)_L$ quintuplet fermions with additional quadruplet scalars [9, 10] can also give rise to interesting signatures at the collider experiments. But, in this case, the neutral component of the quintuplet fermion is stable only over a very finely tuned region of the parameter space.

An alternate solution is to instead introduce a left-right symmetric (LRS) framework [11, 12] with a quintuplet being charged under $SU(2)_R$. LRS models with the gauge group extended to $SU(3)_C \times SU(2)_L \times SU(2)_R \times U(1)_{B-L}$ are one of the most well motivated extensions of the SM for a number of reasons. Firstly, they can explain the origin of parity violation observed in the SM as a symmetry broken spontaneously at some high scale. The conservation of parity (P) symmetry at high scale forbids P-violating terms in the QCD Lagrangian [13–21] and hence, can naturally solve the strong-CP problem without introducing a global Peccei-Quinn symmetry [22]. Moreover, the presence of a right-handed neutrino in the particle spectrum is essentially governed by the gauge structure and hence, naturally explaining the origin of light neutrino masses.

In this work, we consider $SU(3)_C \times SU(2)_L \times SU(2)_R \times U(1)_{B-L}$ gauge symmetry and introduce a vector-like fermion multiplet which is a quintuplet under $SU(2)_R$ and singlet under $SU(2)_L$. We also introduce a scalar multiplet which is doublet under $SU(2)_R$ to break $SU(2)_R \times U(1)_{B-L} \to U(1)_Y$ and a scalar bidoublet to break the electroweak symmetry, $SU(2)_L \times U(1)_Y \to U(1)_{EW}$. In this scenario, the hypercharge quantum number is a derived quantity and allows for many different combinations of charge assignment for the quintuplet including the possibilities of having a neutral component which could be good candidate for dark matter. The dark matter phenomenology of this particular scenario was studied in details in refs. [1, 3]. It was shown in ref. [3] that in the presence of a singlet scalar, an $SU(2)_R$ quintuplet fermion with neutral state mass even as low as 100 GeV can explain the observed relic density (RD) data and is also consistent with DM direct detection experiments.

The tree-level masses of the quintuplet particles are still degenerate. However, the mass degeneracy among the quintuplet fermions of different charges are now lifted at the right-handed symmetry breaking scale (heavy right-handed gauge bosons are running in the loops) resulting in much larger mass splitting among them. In particular, the mass splitting maximizes for $(B - L) = 4$ (see ref. [3]) resulting into relatively harder leptons and jets at the collider experiments. In this work, we study the production and subsequent decay of the high charge-multiplicity components of the quintuplet for $(B - L) = 4$ at the LHC experiment. We focus our study in the same-sign lepton (SSL) channels at the 13 TeV LHC. The main advantage of SSL channels at LHC is that these channels are less background prone. The SSL channels carry distinct features of Supersymmetry and many other models as referred in several studies [23–26]. ATLAS and CMS have so far looked

JHEP01(2019)080

in SSL channels in different context, see for example refs. [27, 28]. We have seen that when the neutral component's mass is small, the leptons are soft due to the small mass difference among the components of the quintuplets. Soft leptons also appear in different supersymmetric searches [29–31]. Also, soft leptons in 2-opposite sign same flavor channel has been studied in ref. [32], where the leading and subleading electrons and muons are required to satisfy $p_T \geq 5\,\text{GeV}$.

Rest of this paper is organized as follows. In section 2, we briefly introduce the model. Production and subsequent decays of the charged components of the quintuplet fermions are discussed in section 3. In section 4, we discuss the two, three, and four same-sign multilepton signatures (2SSL, 3SSL, and 4SSL) and the corresponding SM backgrounds at the LHC. We also present the exclusion limit and discovery reach at the 13 TeV LHC for SSL channels in detail. Finally, we conclude in section 5 with discussions.

2 Quintuplet dark matter model

The gauge group in left-right symmetric models is extended to $\text{SU}(3)_C \times \text{SU}(2)_L \times \text{SU}(2)_R \times \text{U}(1)_{B-L}$. The matter fermion sector is given as:

$$
\begin{aligned}
Q_L\left(3,2,1,\frac{1}{3}\right) &= \begin{pmatrix} u \\ d \end{pmatrix}_L, & Q_R\left(3,1,2,\frac{1}{3}\right) &= \begin{pmatrix} u \\ d \end{pmatrix}_R, \\
[4pt] l_L\,(1,2,1,-1) &= \begin{pmatrix} \nu \\ e \end{pmatrix}_L, & l_R\,(1,1,2,-1) &= \begin{pmatrix} \nu \\ e \end{pmatrix}_R,
\end{aligned}
\tag{2.1}
$$

where, the numbers in the bracket corresponds to $\text{SU}(3)_C$, $\text{SU}(2)_L$, $\text{SU}(2)_R$ and $\text{U}(1)_{B-L}$ quantum numbers respectively. Here we see that all the quarks and leptons are a part of either left-handed or right-handed doublets. For any particle in this model, the electric charge Q is given as: $Q = T_L^3 + T_R^3 + Q_{(B-L)}/2$, where $T_{L/R}^3$ represents the third component of the isospin for $\text{SU}(2)_{L/R}$. An additional singlet fermion $N(1,1,1,0)$ is also introduced to generate the light neutrino mass through inverse seesaw mechanism [33–38].

To break the right-handed symmetry, electroweak (EW) symmetry and to generate the quark and lepton masses and mixing, a minimal scalar Higgs sector is required and given by,

$$
H_R(1,1,2,1) = \begin{pmatrix} H_R^+ \\ H_R^0 \end{pmatrix}, \qquad \Phi(1,2,2,0) = \begin{pmatrix} \phi_1^0 & \phi_2^+ \\ \phi_1^- & \phi_2^0 \end{pmatrix}. \tag{2.2}
$$

The non-zero vacuum expectation values (VEV) of the scalar fields are $\langle H_R^0 \rangle = v_R$, $\langle \phi_1^0 \rangle = v_1$ and $\langle \phi_2^0 \rangle = v_2$. The VEV of the doublet v_R is responsible for breaking the right-handed symmetry while bidoublet VEVs v_1 and v_2 break the EW symmetry.

One can thus obtain the charged gauge boson mass-squared matrix (M_W^2) in the basis ($W_R^\pm, W_L^\pm$) and the neutral gauge boson mass-squared matrix (M_Z^2) in the basis

(W_R^3, W_L^3, V) as:

$$M_W^2 = \frac{1}{2}\begin{bmatrix} g_R^2\left(v_R^2+v^2\right) & g_L g_R v_1 v_2 \\ g_L g_R v_1 v_2 & g_L^2 v^2 \end{bmatrix}, \quad M_Z^2 = \frac{1}{2}\begin{bmatrix} g_R^2\left(v_R^2+v^2\right) & g_L g_R v^2 & -g_R g_{B-L} v_R^2 \\ g_L g_R v^2 & g_L^2 v^2 & 0 \\ -g_R g_{B-L} v_R^2 & 0 & g_{B-L}^2 v_R^2 \end{bmatrix}, \tag{2.3}$$

where, $v^2 = v_1^2 + v_2^2$ is the EW VEV $\sim 174\,\text{GeV}$ while g_L, g_R and g_{B-L} are the $\text{SU}(2)_L$, $\text{SU}(2)_R$ and $\text{U}(1)_{B-L}$ gauge couplings respectively. Our model corresponds to a LRS scenario where the parity and right-handed symmetry breaking scales are decoupled [39]. This is evident from the fact that our scalar spectrum does not contain a left-handed doublet, and hence the left and right-handed gauge couplings may not be the same. Thus, neglecting the left-right mixing, the new right-handed heavy gauge bosons masses are:

$$M_{W_R}^2 = \frac{1}{2} g_R^2\left(v_R^2+v^2\right), \quad M_{Z_R}^2 = \frac{1}{2}\left(g_R^2+g_{B-L}^2\right)\left[v_R^2 + \frac{g_R^2 v^2}{\left(g_R^2+g_{B-L}^2\right)}\right]. \tag{2.4}$$

The left-handed W and Z boson masses are given by their usual expression in the SM with the identification of the effective hypercharge gauge coupling as,

$$g_Y = \frac{g_R\, g_{B-L}}{\sqrt{\left(g_R^2+g_{B-L}^2\right)}}. \tag{2.5}$$

The right-handed VEV needs to be quite high so as to get a large enough Z_R mass in order to avoid direct detection constraints for dark matter. As can be seen from figure 5 of ref. [3], the mass of the Z_R boson should be at least 7 TeV to circumvent the direct detection constraints for a dark matter mass of 150 GeV. Since we have considered a parameter space with the lowest value of quintuplet dark matter mass of 150 GeV for our collider analysis, this limit needs to be satisfied. For this reason, we choose $v_R = 13\,\text{TeV}$, which gives $M_{W_R} = 6.0\,\text{TeV}$ and $M_{Z_R} = 7.14\,\text{TeV}$.

Motivated by Minimal Dark Matter models, we consider an $\text{SU}(2)_R$ vector-like fermion quintuplet, which can accommodate the dark matter. We represent the quintuplet as,

$$\chi(1,1,5,X) = (\chi^{2+X/2}, \chi^{1+X/2}, \chi^{X/2}, \chi^{-1+X/2}, \chi^{-2+X/2})^T, \tag{2.6}$$

where $X = 0, 2, 4$ are its possible $(B-L)$ quantum numbers. The neutral component of χ can be a viable dark matter while its charged components can be produced at the colliders. The couplings of the gauge bosons (Z, Z_R, W_R and photon) with the quintuplet fields are,

$$\begin{aligned}\mathcal{L}_{\text{gauge}} \supset & -\frac{g_Y^2}{\left(g_R^2+g_Y^2\right)} Q_{\chi^i}\overline{\chi}^i Z^\mu\ \gamma_\mu\ \chi^i + e\ Q_{\chi^i}\overline{\chi}^i A^\mu \gamma_\mu\ \chi^i \\ & + \sqrt{g_R^2 - g_Y^2}\left[Q_{\chi^i} - \frac{g_R^2 Q_{B-L}}{2\left(g_R^2-g_Y^2\right)}\right]\overline{\chi}^i Z_R^\mu \gamma_\mu \chi^i + \left(\frac{g_R}{\sqrt{2}} r_Q \overline{\chi}^{i+1}\ W_R^\mu\ \gamma_\mu\ \chi^i + h.c.\right).\end{aligned} \tag{2.7}$$

JHEP01(2019)080

Here

$$r_Q = \sqrt{(3 + Q_{\chi_i} - Q_{B-L}/2)(2 - Q_{\chi_i} + Q_{B-L}/2)} \tag{2.8}$$

and χ^i represents the component of the quintuplet χ with electric charge $Q_{\chi^i} = i$.

The fermion masses are generated as the bidoublet fields get non-zero VEV and the corresponding Yukawa Lagrangian is given as:

$$\begin{aligned}\mathcal{L}_Y = &\left(Y_q \overline{Q}_L \Phi Q_R + \widetilde{Y}_q \overline{Q}_L \widetilde{\Phi} Q_R + Y_l \bar{l}_L \Phi l_R + \widetilde{Y}_l \bar{l}_L \widetilde{\Phi} l_R + f_R \bar{l}_R \widetilde{H}_R N + H.C.\right) \\ &+ \frac{\mu_N}{2} NN + M_\chi \overline{\chi}\chi\,,\end{aligned} \tag{2.9}$$

where Y and f are the Yukawa couplings and $\widetilde{\Phi} = \tau_2 \Phi^* \tau_2$, $\widetilde{H}_R = i\tau_2 H_R^*$. Hence, the quark and charged lepton masses are:

$$M_u = Y_q v_1 + \widetilde{Y}_q v_2, \quad M_d = Y_q v_2 + \widetilde{Y}_q v_1, \quad M_l = Y_l v_2 + \widetilde{Y}_l v_1. \tag{2.10}$$

We choose a large $\tan\beta$ $(= v_1/v_2)$ limit so that $Y_{33}^q \sim 1$ for the top quark mass while $\widetilde{Y}_{33}^q < 10^{-2}$. A smaller value of $\tan\beta$ would require a larger value of Y_{33} in general, leading to the top Yukawa becoming non-perturbative at relatively lower mass scales. The neutrinos get masses through the inverse seesaw mechanism with the 3×3 mass matrix in the basis (ν_L, ν_R, N) given as:

$$M_\nu = \begin{bmatrix} 0 & m_D & 0 \\ m_D^T & 0 & f_R v_R \\ 0 & f_R^T v_R & \mu_N \end{bmatrix}, \tag{2.11}$$

where $m_D = Y_l v_1 + \widetilde{Y}_l v_2$ is the neutrino Dirac mass term. Assuming $f_R v_R \gg m_D, \mu_N$, the approximate expressions for the neutrino mass eigenvalues (for one generation) are,

$$m_{\nu_1} \sim \frac{(f_R^{-1} M_D^T)^T \mu_N (f_R^{-1} M_D^T)}{v_R^2}, \qquad m_{\nu_{2,3}} \sim f_R v_R. \tag{2.12}$$

So in this framework, light neutrino masses can be easily generated by appropriate choice of parameters.

The quintuplet fermion in this model can have a few different values of $(B-L)$ quantum numbers (0, 2, and 4) but for our study we will only consider the case with $(B - L) = 4$. This scenario will have highest charge multiplicity particles, hence gives rise to interesting collider signatures. Component fields of the $\mathrm{SU}(2)_R$ quintuplet for $(B - L) = 4$ can be expressed as,

$$\chi(1, 1, 5, 4) = \left(\chi^{++++}, \chi^{+++}, \chi^{++}, \chi^{+}, \chi^{0}\right)^T. \tag{2.13}$$

For brevity, we will denote $\chi^{\pm\pm\pm\pm}$ as $\chi^{4\pm}$, $\chi^{\pm\pm\pm}$ as $\chi^{3\pm}$, and $\chi^{\pm\pm}$ as $\chi^{2\pm}$ from here onwards. It is evident from eq. (2.9), that all components (χ^i) of the quintuplet are degenerate in mass at the tree level. Their masses are all equal to M_χ as given in eq. (2.9). The mass splitting

JHEP01(2019)080

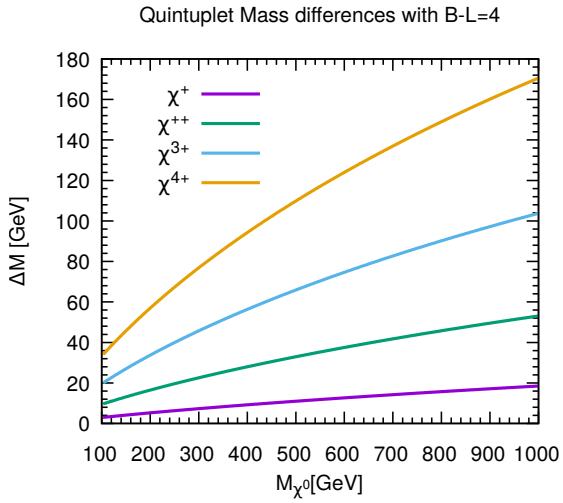

Figure 1. Mass difference between various charged states as a function of the neutral state's mass for $(B-L)=4$ case, assuming M_{W_R}= 6 TeV and M_{Z_R}= 7.14 TeV (see eq. (2.14)).

between the various charged states are generated by the radiative corrections given as:

$$M_{\chi^i}-M_{\chi^0} = \frac{g_R^2}{(4\pi)^2}M_{\chi^0}\Bigg[Q_{\chi^i}\left(Q_{\chi^i}-Q_{B-L}\right)f(r_{W_R})-Q_{\chi^i}\left(\frac{\sqrt{g_R^2-g_Y^2}}{g_R^2}Q_{\chi^i}-Q_{B-L}\right)f(r_{Z_R}) \\ -\frac{g_Y^2}{g_R^2}Q_{\chi^i}^2\left\{s_W^2 f(r_Z)+c_W^2 f(r_\gamma)\right\}\Bigg], \tag{2.14}$$

where $r_X = m_X/M_{\chi^0}$, $f(r) \equiv 2\int_0^1 dx(1+x)\log\left[x^2+(1-x)r^2\right]$ and Q_{χ^i} is the electric charge of χ^i. To calculate the mass splittings, we have chosen the value of $g_R = 0.653$ at the scale of Z_R boson mass. This is merely a choice in our parameter region. In the limit of small left-right mixing, the value of $g_L = 0.653$ at the electroweak scale is determined by the measured values of α_{EM} and weak mixing angle θ_W. The mass splitting between the various charged states of the quintuplet as a function of the neutral quintuplet mass has been shown in figure 1 for the case with $(B-L) = 4$. The mass difference between the components of the quintuplets increase with their mass. In order to satisfy the correct RD, one needs to introduce a singlet scalar as shown in ref. [3]. The same paper also has in-depth discussion of the model, dark matter phenomenology and collider phenomenology of the singlet scalar. In this work, we are interested in the collider signatures of the quintuplet fermions at the LHC which will be discussed in the following sections.

3 Production and decay of multi-charged quintuplet fermions

The quintuplet, being charged under $SU(2)_R$ and $U(1)_{B-L}$, has gauge interaction with photon, SM Z boson, Z_R and $W_R^\pm$ (see eq. (2.7)).[1] Therefore, the quintuplet fermions can

[1]The couplings of the quintuplet fermions with the SM $W^\pm$ is suppressed by small $W_L^\pm$–$W_R^\pm$ mixing.

JHEP01(2019)080

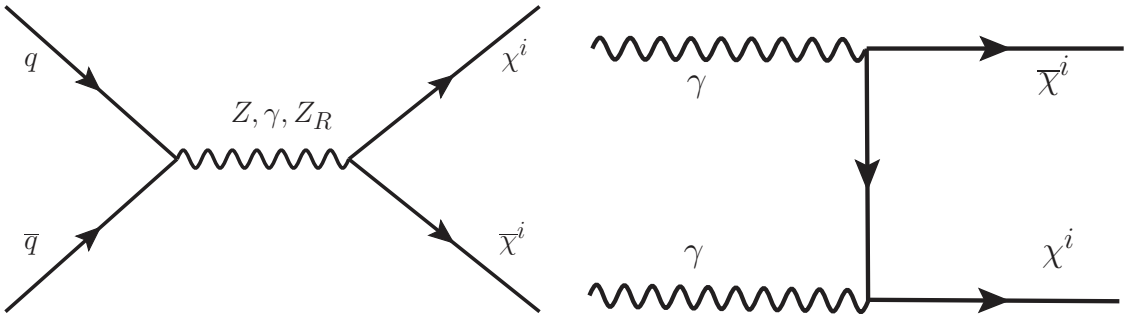

Figure 2. The left panel shows the Feynman diagram for the s-channel Drell-Yan pair-production of the quintuplet fermion. The right panel portrays the Photo production of $\chi^i\overline{\chi}^i$ through t-channel photon-photon fusion process.

be pair-produced at the LHC via quark-antiquark initiated Drell-Yan (DY) process with a photon/Z/Z_R in the s-channel as shown in the left panel of figure 2. The electrically charged components of the quintuplet (χ) can also be produced from photon-photon fusion in the initial state ($\gamma\gamma \to \chi^i\overline{\chi}^i$), where $i = 4$, 3, 2, and 1. The right panel of figure 2 shows a representative diagram of the photon-photon fusion process for the pair-production of $\chi^i\overline{\chi}^i$. Photo production of $\chi^{i\pm}\chi^{i\mp}$ pairs takes place via a t or a u channel exchange of a $\chi^{i\pm}$ and hence, is not suppressed by the parton center of mass energy. Moreover, the coupling of photon with a pair of $\chi^{i\pm}$ being proportional to its charge (i), the matrix element squared of photo productions are enhanced by a factor of i^4. However, the photo-production of charged fermions at the LHC is suppressed by the small parton density of photon inside a proton. To denote the charge multiplicity of the quintuplet in the following, we adopt the notation $\chi^{n\pm}$, where n runs from 0 to 4.

In fact, the parton density of the photon is so small that most of the older versions of PDF's do not include photon as a parton. However, if we want to include QED correction to the PDF, inclusion of the photon as a parton with an associated parton distribution function is necessary. In the era of precision physics at the LHC when PDF's are determined upto NNLO in QCD, NLO QED corrections are important (since α_s^2 is of the same order of magnitude as α) for the consistency of calculations. Moreover, as discussed previously, photon-initiated processes could become significant at high energies for some processes. In view of these facts, NNPDF [40, 41], MRST [42] and CTEQ [43] have already included photon PDF into their PDF sets.

In order to compute the cross-sections and generate events at the LHC, we incorporate the model Lagrangian of eq. (2.7) in FeynRules (v2.3.13) [44, 45]. We implement the couplings for each component of the quintuplet (i =0, 1, 2, 3, 4) with the gauge bosons, derived from eq. (2.7). Using FeynRules we generate the model file for MadGraph5_aMC@NLO (v2.2.1) [46]. For the cross-sections, we use the NNPDF23LO1 parton distributions [47] with the factorization and renormalization scales kept fixed at the central m_T^2 scale after k_T-clustering of the event. The quark-antiquark initiated DY production cross-section for the $\chi^{4+}\chi^{4-}$ pairs are presented in figure 3 (right panel) at the LHC with 13 TeV center of mass energy. Being s-channel, DY pair-production cross-sections are significantly

JHEP01(2019)080

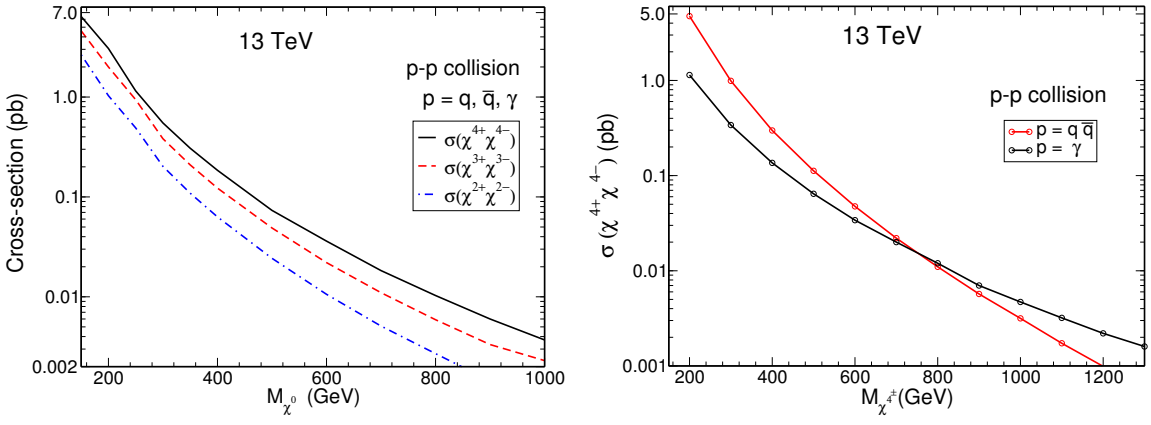

Figure 3. Left panel shows the total cross-section of different production modes as a function of the neutral component's mass (M_{χ^0}) at 13 TeV when both quarks and photons are considered at the initial states. The cross-section of other production modes are negligible. In the right panel, we give the cross-sections to produce a pair of quadruply charged particles as a function of its mass ($M_{\chi^{4\pm}}$) at 13 TeV. We show it separately for two different initial states (quark-antiquark and photons).

Process	Cross-section (pb)	Process	Cross-section (pb)
$pp \to \chi^{4+}\chi^{4-}$	0.1843	$pp \to \chi^{4+}\chi^{3-}$	0.00058
$pp \to \chi^{3+}\chi^{3-}$	0.1225	$pp \to \chi^{3+}\chi^{2-}$	0.00088
$pp \to \chi^{2+}\chi^{2-}$	0.0630	$pp \to \chi^{2+}\chi^{1-}$	0.00078
$pp \to \chi^{1+}\chi^{1-}$	0.0174	$pp \to \chi^{1+}\chi^{0}$	0.00052

Table 1. Cross-sections at the 13 TeV LHC in different production channels when $M_{\chi^{n\pm}} = [400,409,428,456,494]$ GeV ($n = 0$ to 4), and initial state partons and photons both are considered, $p = \gamma, q, \bar{q}$. The contribution from $pp \to \chi^0\chi^0$ is negligible.

suppressed for larger $\chi^{4\pm}$ masses. In figure 3 (right panel), we also present the photo-production cross-section of $\chi^{4\pm}\chi^{4\mp}$ pairs as a function of $\chi^{4\pm}$ mass ($M_{\chi^{4\pm}}$) at the 13 TeV LHC. It shows that photon-photon fusion contributes significantly for $M_{\chi^{4\pm}} < 800$ GeV and for $M_{\chi^{4\pm}} > 800$, photo-production dominates over the DY contribution. In the left panel of figure 3 we present the total (DY+photo-production) pair-production cross-sections for $\chi^{4\pm}\chi^{4\mp}$, $\chi^{3\pm}\chi^{3\mp}$, and $\chi^{2\pm}\chi^{2\mp}$ as a function of M_{χ^0} at the LHC with $\sqrt{s} = 13$ TeV. The total pair-production cross-sections varies between a few pb to a few fb as we vary the χ^0 mass between 200 GeV to 1 TeV. Quintuplet fermions can also be produced in association with another quintuplet fermion from quark-antiquark initial state via a $W_R^\pm$ exchange in the s-channel. However, associated production cross-sections are suppressed by the mass of the $W_R^\pm$ in the s-channel. In table 1, we present the numerical values of pair and associated production cross-sections for a particular benchmark point.

After being produced at the LHC, the quintuplet fermions undergo a tree-level 3-body decay into a lighter component and a pair of SM quarks or leptons. χ^0 being stable remains invisible in the detector. Therefore, the pair/associated production of the quintuplet fermions gives rise to multiple-jets and/or leptons (including the same-sign multileptons)

JHEP01(2019)080

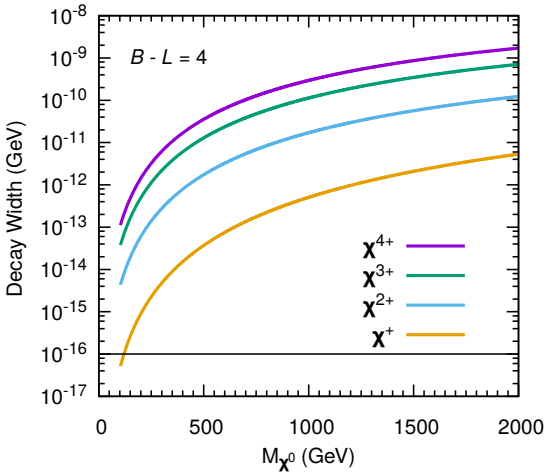

Figure 4. Total decay width of the charged states a function of the neutral state's mass for $(B - L) = 4$ case, assuming M_{W_R}= 6 TeV and M_{Z_R}= 7.14 TeV. If the decay width is less than 10^{-16} GeV, the particle decays outside the detector.

and missing transverse energy signature at the LHC. However, the 3-body decay of the quintuplet fermions proceed through an off-shell $W_R^{\pm}$ boson with a mass of few TeV. Therefore, before going into the details of signal and background analysis, it is important to compute the decay width of the quintuplet fermions to ensure that they decay inside the detector. For a particle having a decay width less than 10^{-16} GeV, it will escape the detector before it can decay. We can see from figure 4 that the decay widths of all the charged fermions in the $(B - L) = 4$ quintuplet are always larger than 10^{-16} GeV, which ensures that they will decay inside the detector. If the decay width of the charged fermions fall in the range around 10^{-13} to 10^{-16} GeV, then there may be a possibility to see the displaced vertex signature as well. For a major part of the parameter space considered in this paper, the decay widths of $\chi^{2\pm}$, $\chi^{3\pm}$, and $\chi^{4\pm}$ are always above 10^{-13} GeV (see figure 4). Therefore, we do not explore the possibility of displaced vertex signature in this work.

If a charged ($n = 1, 2, 3, 4$) component of the quintuplet ($\chi^{n\pm}$) is produced, it will form a cascade of decay via the process discussed above. For example, the main contribution in the 4 same-sign lepton channel (4SSL) will come from the production $pp \to \chi^{4+}\chi^{4-}$, and the decays of χ^{4+} and χ^{4-}, as shown in figure 5. Other components of the quintuplet can also decay in the same manner and depending on the decay pattern there can be interesting collider signatures in the same-sign lepton (SSL) and other multilepton channels. In this study, we focus mainly on 2, 3, and 4 same-sign multilepton signals (2SSL, 3SSL, and 4SSL).

4 Collider signature of quintuplets

As discussed in the previous section, the production and decay of the quintuplet fermions give rise to multiple leptons/jets in association with missing transverse energy signatures at the LHC. For example, the production of $\chi^{4\pm}\chi^{4\mp}$ pairs could result into 0 to 8 leptons

JHEP01(2019)080

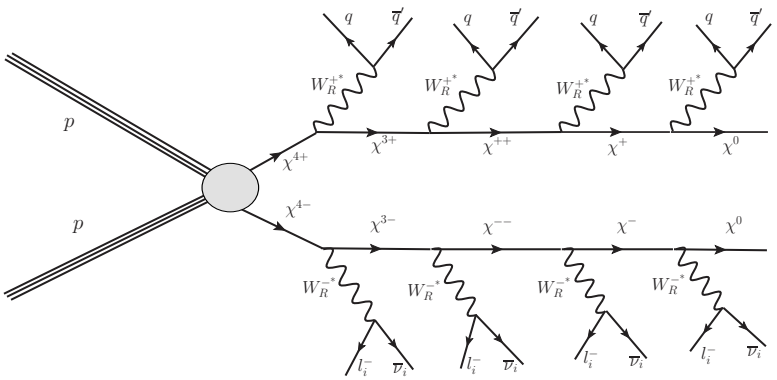

Figure 5. Cascade decay of $\chi^{4\pm}$ into leptons ($l = e, \mu$) and jets, contributing to the 4SSL channel.

$M_{\chi^{n\pm}}$ (GeV)	$\sigma\times$BR(fb)(2SSL)	$\sigma\times$BR(fb)(3SSL)	$\sigma\times$BR(fb)(4SSL)
150,154,163,177,195	886.5	132.54	24.17
200,205,216,233,257	214.4	71.88	11.55
250,256,269,289,317	147.1	32.45	6.0
300,307,322,345,377	75.83	11.23	2.0
350,358,375,401,436	41.35	6.21	1.16
400,409,428,456,494	24.73	3.7	0.7

Table 2. Signal cross-sections (production cross-section × effective BR) in the 2SSL, 3SSL, and 4SSL channels at the 13 TeV LHC for different masses of the quintuplet. Here n runs from 0 to 4 for a given quintuplet. This cross-sections are obtained considering both quarks and photons in the initial state. We consider BR($\chi^{Q+1} \to l\nu\chi^{Q}$) = 0.22 ($l = e, \mu$), and BR($\chi^{Q+1} \to q\bar{q}\chi^{Q}$) = 0.67.

(including same-sign 2, 3, and 4 leptons) in the final state depending on the decay cascade of $\chi^{4\pm}$. Fully leptonic/hadronic decay cascade of both $\chi^{4\pm}$ results into 8/0 leptons signature. Whereas, leptonic decay cascade (fully or partially) for one $\chi^{4\pm}$ and hadronic decay cascade of the other $\chi^{4\mp}$ give rise to four same-sign leptons in the final state. The pair and associated production of all combinations of $\chi^{4\pm}, \chi^{3\pm}$, and $\chi^{2\pm}$ contribute in the 2SSL channel. For the 3SSL channel, $\chi^{4+}\chi^{4-}$, $\chi^{3+}\chi^{3-}$, $\chi^{4+}\chi^{3-}$, and $\chi^{3+}\chi^{2-}$ contribute, but for the 4SSL channel the signal stems only from $\chi^{4+}\chi^{4-}$ and $\chi^{4+}\chi^{3-}$. The cross-section (σ) × effective Branching Ratio (BR) in different SSL channels are listed in table 2 for a few selected masses of the quintuplet. The simulation of production and decay of the quintuplet fermion pairs at the LHC are discussed in the following section.

4.1 Event generation and simulation

The signal events for the production of the quintuplets are simulated using MadGraph [46, 48] and showered with PYTHIA [49]. After that, the events are passed through DELPHES 3 [50] for detector simulation. In DELPHES, we choose the isolation cut for leptons to be $\Delta R_{\rm max} = 0.5$ while reconstructing the events. This requirement ensures no

JHEP01(2019)080

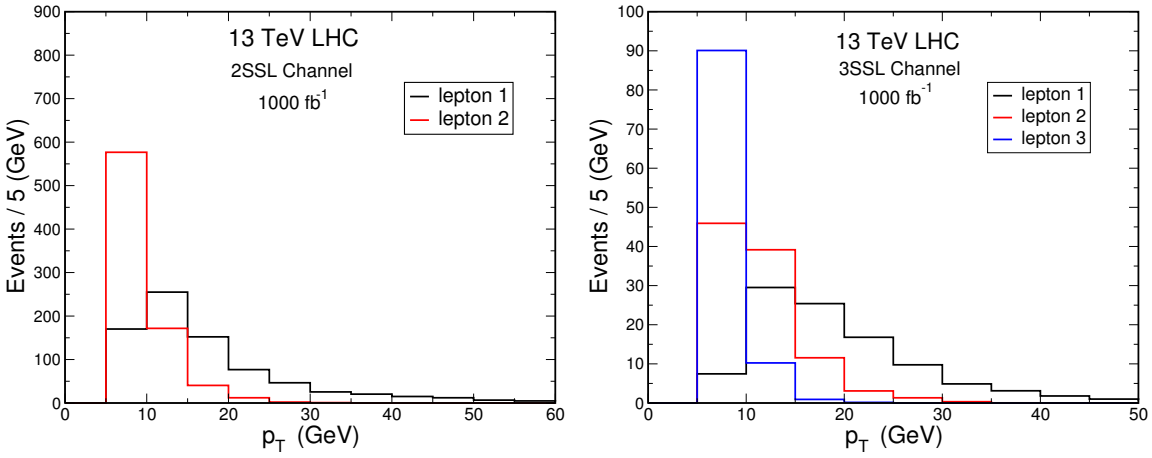

Figure 6. The left panel shows the distributions of the leading and subleading lepton transverse momentum ($p_T(l)$) for signal events in the 2SSL channel at the 13 TeV LHC. The right panel depicts the same in the 3SSL channel. Here leptons are $l = e, \mu$. In both the panels, the events are weighted at 1000 fb^{-1}.

hadronic activity inside this isolation cone. The isolation cut reduces the SM background of the leptons coming from the decays of B-mesons. The probability of a jet to be misidentified as a lepton is taken as a modulo inside DELPHES [51]. In our model, leptons get produced from the decay of a heavier component of the quintuplet to a lighter component. As discussed earlier, small mass splitting between different components of the quintuplet results in soft leptons. For such soft leptons the charge misidentification probability is small and hence neglected.

The leading SM backgrounds for 2SSL are $t\bar{t}$, ZZ, WZ, WW, $t\bar{t}W$, $t\bar{t}Z$, $t\bar{t}h$, and hZ. Semileptonic decay of $t\bar{t}$ contributes to the 2SSL when the b-quark generated from decay of top quark further decays leptonically. On the other hand, di-boson production contributes to the 2SSL channel if one or more leptons from the leptonic decay of the SM bosons fall outside the detector coverage (leptons are too soft or they fall in the high rapidity region). Here, $b\bar{b}W$ could also contribute when one lepton results from the $W^{\pm}$ decay and the other lepton with same electric charge arises from leptonic B-meson decays. Among the above mentioned backgrounds, the dominant contribution in 2SSL channel comes from WZ, ZZ, and $t\bar{t}W$. In the 3SSL channel, following SM backgrounds are considered: $t\bar{t}W$, $t\bar{t}Z$, $t\bar{t}h$, WWZ, WZZ, ZZZ, $t\bar{t}t\bar{t}$, and $t\bar{t}b\bar{b}$. Out of all these possibilities, major contributions come from $t\bar{t}W$ and WZZ. All background events are generated using MadGraph and the cross-sections are taken upto NLO (see refs. [52–59]).

4.2 Event selection

Following are the generator level acceptance cuts that we impose while simulating the signal and backgrounds.

- For any lepton: $p_T\,(e, \mu) > 6\,\text{GeV}$.
- For any jet: $p_T\,(j) > 20\,\text{GeV}$.

JHEP01(2019)080

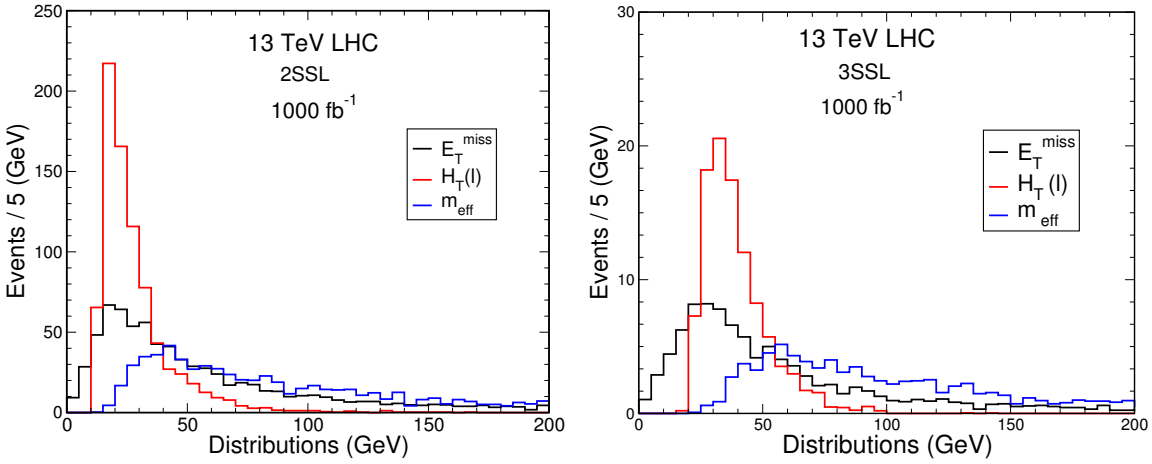

Figure 7. The left panel shows the distributions of the missing energy ($E_T^{\rm miss}$), sum of the lepton transverse momentum ($H_T(l) = \sum_i p_T(l_i)$), and effective mass ($m_{\rm eff} = E_T + H_T(l) + H_T(j)$) for signal events in the 2SSL channel at the 13 TeV LHC. The right panel depicts the same in the 3SSL channel. Here leptons are $l = e, \mu$. In both the panels, the events are weighted at 1000 fb^{-1}.

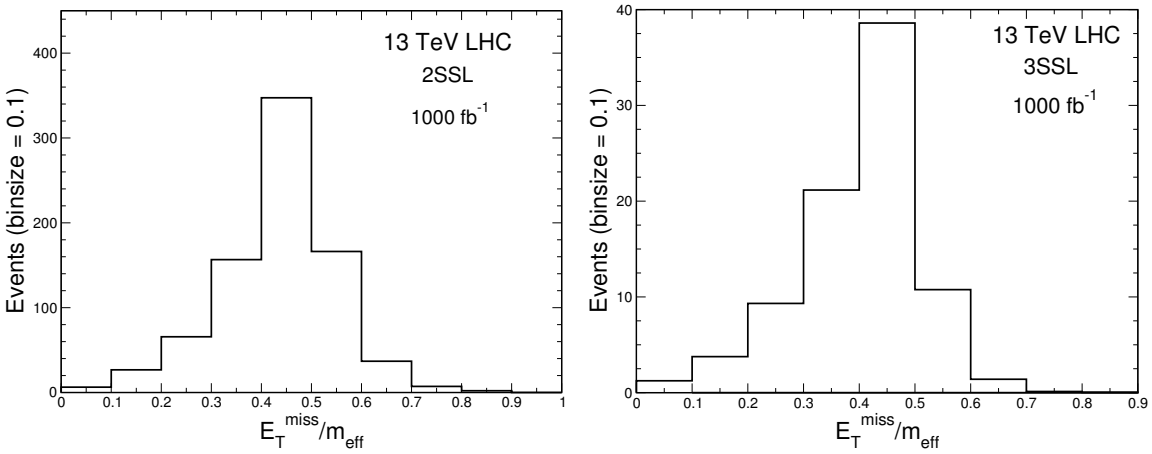

Figure 8. The distribution of the ratio of the missing energy and the effective mass ($E_T^{\rm miss}/m_{\rm eff}$) for signal events in the 2SSL (left panel) and 3SSL (right panel) channels at the 13 TeV LHC. The events are weighted for 1000 fb^{-1}.

- $|\eta(e)| < 2.5$, $|\eta(\mu)| < 2.5$, and $|\eta(j)| < 2.4$.

- $\Delta R_{l,l'} > 0.2$ $(l, l' = e, \mu)$, $\Delta R_{j,j} > 0.5$, and $\Delta R_{\ell,j} > 0.4$.

The transverse momentum distributions for the leading and subleading signal leptons are given in figure 6 (left panel for 2SSL and right panel for 3SSL). It is evident from this figure that the signal leptons are soft, as discussed earlier. Since most of the signal events are distributed in the lower p_T region, a cut on the upper limit of $p_T(l)$ will effectively reduce the background. The other kinematic variables considered in the study are the sum of the

JHEP01(2019)080

Selection Cuts	2SSL	3SSL	4SSL
$S1$	l^+l^+ or l^-l^-	$l^+l^+l^+$ or $l^-l^-l^-$	$l^+l^+l^+l^+$ or $l^-l^-l^-l^-$
$S2$	$b-jets=0$	$b-jets=0$	$b-jets=0$
	$p_T(l_1)<35\,\text{GeV}$	$p_T(l_1)<35\,\text{GeV}$	$p_T(l_1)<35\,\text{GeV}$
	$p_T(l_2)<20\,\text{GeV}$	$p_T(l_2)<20\,\text{GeV}$	$p_T(l_2)<20\,\text{GeV}$
	$E_T^{\text{miss}}/m_{\text{eff}}>0.2$	$p_T(l_3)<15\,\text{GeV}$	$p_T(l_3)<15\,\text{GeV}$
	$H_T(l)<60\,\text{GeV}$	$E_T^{\text{miss}}/m_{\text{eff}}>0.2$	$p_T(l_4)<15\,\text{GeV}$
	$H_T(j)<200\,\text{GeV}$	$H_T(l)<60\,\text{GeV}$	$E_T^{\text{miss}}/m_{\text{eff}}>0.2$
		$H_T(j)<200\,\text{GeV}$	$H_T(l)<60\,\text{GeV}$
			$H_T(j)<200\,\text{GeV}$
$S3_x$	$m_T<40\,\text{GeV}$	-	-
	$E_T^{\text{miss}}>10\,\text{GeV}$	-	-
$S3_y$	$m_T<40\,\text{GeV}$	-	-
	$E_T^{\text{miss}}>20\,\text{GeV}$	-	-
$S3_z$	$m_T<40\,\text{GeV}$	-	-
	$E_T^{\text{miss}}>30\,\text{GeV}$	-	-

Table 3. Selection criteria ($S1$, $S2$, and $S3$) that we consider for the 2SSL, 3SSL, and 4SSL channels. In selection $S1$, we only consider the events with exactly 2, 3 or 4 leptons with same sign. Other events containing opposite sign leptons are vetoed. Here $l=e,\mu$. Also, note that for the 3SSL and 4SSL channels, we do not impose selection criteria $S3$.

transverse momentum of the leptons and jets, and the effective mass which are defined as:

$$H_T(l)=\sum_i p_T(l)_i, \quad H_T(j)=\sum_i p_T(j)_i, \quad m_{\text{eff}}=E_T+H_T(l)+H_T(j). \tag{4.1}$$

The distributions of the E_T^{miss}, $H_T(l)$, and m_{eff} are shown in figure 7 for the 2SSL (left panel) and 3SSL (right panel) channel. We find that an upper limit on $H_T(l)$ and $H_T(j)$ help to reduce the backgrounds significantly. In figure 8, we plot distribution of the $E_T^{\text{miss}}/m_{\text{eff}}$ for both the channels. In the next section, we find that a cut on the lower values of the $E_T^{\text{miss}}/m_{\text{eff}}$ turns out to be quite effective to reduce the QCD-jet backgrounds. The backgrounds from $t\bar{t}W$ and $t\bar{t}Z$ can be reduced by applying a b-jet veto. Another effective way to reduce the same-sign multilepton backgrounds is to consider only small values of the transverse mass (m_T). We imposed further selection criteria on these kinematic variables to enhance the signal to background ratios in the 2SSL, 3SSL, and 4SSL channels. The final event selection criteria are listed in table 3 and the effects are discussed in the next section.

4.3 Exclusion limits and discovery reach in the same-sign multilepton channels

As discussed in table 3, the same-sign lepton ($l=e,\mu$) final states are required to pass the selections $S1$, $S2$, and $S3$ in the 2SSL channel. For 3SSL, and 4SSL channels we only

JHEP01(2019)080

impose $S1$ and $S2$. While analyzing the same-sign multilepton channels, we find that the remaining background is small after passing through several selections. If the background is small then the standard formula ($s/\sqrt{b}$) overestimates the discovery significance. Also, in real experiments, the background (b) is never known with 100% accuracy. Therefore, while calculating the discovery significance and exclusion, we include an uncertainty in the background (Δ_b) [60]. This analysis is helpful to deal with small backgrounds, implemented before in ref. [61]. The significance for discovery is defined as,

$$Z_{\rm dis} = \left[2\left((s+b)\ln\left[\frac{(s+b)(b+\Delta_b^2)}{b^2+(s+b)\Delta_b^2}\right] - \frac{b^2}{\Delta_b^2}\ln\left[1+\frac{\Delta_b^2 s}{b(b+\Delta_b^2)}\right]\right)\right]^{1/2}. \tag{4.2}$$

If $\Delta_b = 0$,

$$Z_{\rm dis} = \sqrt{2[(s+b)\ln(1+s/b) - s]}. \tag{4.3}$$

In the above equation, if b is large, then we obtain the well known expression

$$Z_{\rm dis} = s/\sqrt{b}. \tag{4.4}$$

It is evident from the above discussion that if b is small, $s/\sqrt{b}$ overestimates the significance. Therefore, we use the expression given in eq. (4.2) to estimate the discovery reach by assuming $Z_{\rm dis} \geq 5$ which corresponds to 5σ discovery ($p < 2.86 \times 10^{-7}$). To set the exclusion limit at a given confidence level (CL), we use the following expression

$$Z_{\rm exc} = \left[2\left\{s - b\ln\left(\frac{b+s+x}{2b}\right) - \frac{b^2}{\Delta_b^2}\ln\left(\frac{b-s+x}{2b}\right)\right\} - (b+s-x)(1+b/\Delta_b^2)\right]^{1/2}, \tag{4.5}$$

where

$$x = \sqrt{(s+b)^2 - 4sb\Delta_b^2/(b+\Delta_b^2)}. \tag{4.6}$$

In the above equation, if $\Delta_b = 0$,

$$Z_{\rm exc} = \sqrt{2(s - b\ln(1+s/b))}. \tag{4.7}$$

For a median expected 95% CL exclusion ($p = 0.05$), we use $Z_{\rm exc} \geq 1.645$ for different Δ_b. With increasing amount of LHC data, and hence for a better understanding of the detector response, the experimental uncertainties in the estimation of the SM backgrounds are expected to be reduced significantly. Therefore, we assume that the systematic uncertainty in background estimation falls as $1/\sqrt{\mathcal{L}}$ and we also incorporate this effect in Δ_b. We choose different values of the systematic uncertainties at 10%, 25% and 50% at 10 fb^{-1} integrated luminosity and scale the uncertainty appropriately for higher luminosities.

For the two same-sign lepton channel (2SSL), we require exactly 2 leptons (ee or $\mu\mu$ or $e\mu$). The selection criteria in 2SSL channel are listed in table 3. The signal cross-section after passing various selections ($S1$, $S2$, and $S3$) are given in table 4 for 2SSL channel at the 13 TeV LHC. The signal events suffer from a very low missing transverse energy ($E_T^{\rm miss}$), which comes mainly from the neutral state of the quintuplet (χ^0). So, enforcing a cut on $E_T^{\rm miss}$ will yield smaller signal cross-section, as can be seen in table 4. On the other hand, a

JHEP01(2019)080

$M_{\chi^{n\pm}}$ (GeV)	$\sigma(fb)\times$ BR	$S1$ (fb)	$S2$ (fb)	$S3_x$(fb)	$S3_y$ (fb)	$S3_z$ (fb)
200,205,216,233,257	214.4	2.15	1.88	1.26	0.82	0.48
300,307,322,345,377	75.8	2.22	1.85	1.12	0.77	0.44
400,409,428,456,494	24.7	1.50	1.44	0.58	0.40	0.22
500,511,533,566,610	9.6	0.96	0.61	0.26	0.17	0.09
600,613,638,675,725	4.5	0.61	0.32	0.12	0.08	0.05
700,714,742,783,838	2.3	0.38	0.17	0.05	0.04	0.02
800,816,846,891,950	1.27	0.25	0.10	0.03	0.02	0.01

Table 4. Signal cross-sections after passing the various selection criteria in the 2SSL channel at the 13 TeV LHC for different masses of the quintuplet. Here n runs from 0 to 4 in a given quintuplet. We assume BR($\chi^{Q+1} \to l\nu\chi^{Q}$) = 0.22 where $l = e, \mu$ and BR($\chi^{Q+1} \to q\bar{q}\chi^{Q}$) = 0.67.

Process	Cross-section (fb)	$S1$ (fb)	$S2$ (fb)	$S3_x$ (fb)	$S3_y$ (fb)	$S3_z$ (fb)
$pp \to WW$	130×10^3	0.234	0.117	$< 10^{-4}$	$< 10^{-4}$	$< 10^{-4}$
$pp \to WZ$	49×10^3	98.365	14.56	3.84	2.196	1.124
$pp \to ZZ$	16×10^3	7.303	0.654	0.286	0.182	0.103
$pp \to hh$	40×10^3	0.083	0.012	0.004	0.004	0.003
$pp \to hZ$	0.97×10^3	0.890	0.122	0.046	0.031	0.015
$pp \to t\bar{t}W$	600	1.574	0.014	0.002	0.002	0.002
$pp \to t\bar{t}H$	508	0.503	0.004	$< 10^{-4}$	$< 10^{-4}$	$< 10^{-4}$
$pp \to t\bar{t}Z$	920	0.468	0.002	0.0002	0.0002	0.0002
$pp \to t\bar{t}$	820×10^3	0.369	0.025	$< 10^{-4}$	$< 10^{-4}$	$< 10^{-4}$
Total	-	109.79	15.515	4.176	2.416	1.247

Table 5. Background cross-sections in the 2SSL channel after passing various selection criteria at the 13 TeV LHC.

cut on the lower limit of the missing energy effectively reduces the probability of jet faking leptons in the final state [62]. So, here we choose three different $E_T^{\rm miss}$ cuts, $S3_x$, $S3_y$, and $S3_z$. The background cross-section to pass the same selections are given in table 5 for 2SSL channel. We find that the selection $S3$ is very effective in reducing the backgrounds.

In figure 9 and figure 10, projections of the required luminosity for 95% confidence level exclusion ($Z_{\rm exc} \geq 1.645$) and 5σ discovery ($Z_{\rm dic} \geq 5$) are shown as a function of the neutral state mass (M_{χ^0}), for two different selections $S3_x$ and $S3_z$. To make the predictions we use eq. (4.2) and eq. (4.5) and vary the uncertainty in the backgrounds between $0 - 50\%$. As a larger $E_T^{\rm miss}$ cut further reduces the signal cross-section, more luminosity is expected to be required to set an exclusion in $S3_z$ compared to $S3_x$. But from figure 9, it is clear that the cut on $E_T^{\rm miss}$ is not that sensitive since a strong $E_T^{\rm miss}$ cut also reduces the background cross-section at a comparable rate, as reflected in table 4 and table 5. With 3000 fb^{-1}

JHEP01(2019)080

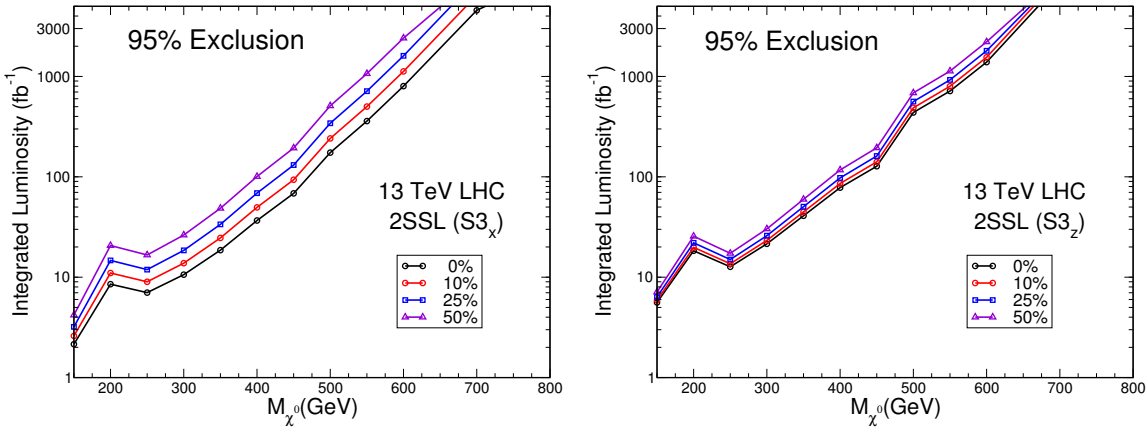

Figure 9. In the left panel, we show the required integrated luminosity for 95% CL exclusion ($Z_{\rm exc} \geq 1.645$) after imposing the $S3_x$ selection criteria in the 2SSL channel at the 13 TeV LHC as a function of M_{χ^0}. The right panel depicts the same for selection criteria $S3_z$. The colored lines in both the panels are for the different level of uncertainties in the background events ranging from 0 to 50%.

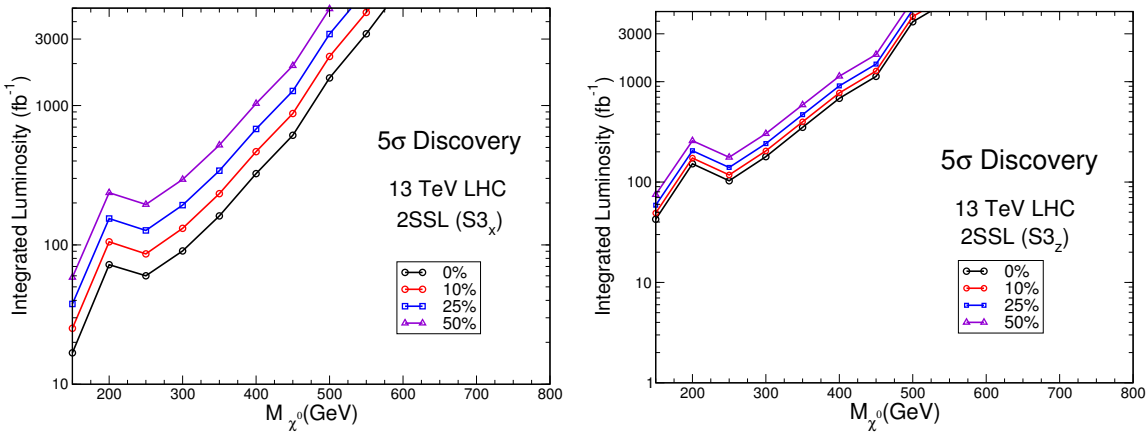

Figure 10. In the left panel, we show the required integrated luminosity for 5σ discovery ($Z_{\rm dis} \geq 5$) after imposing the $S3_x$ selection criteria in the 2SSL channel at the 13 TeV LHC as a function of M_{χ^0}. The right panel depicts the same for selection criteria $S3_z$. The colored lines in both the panels are for the different level of uncertainties in the background events ranging from 0 to 50%.

integrated luminosity, one can exclude up to 610 GeV of the neutral state mass (M_{χ^0}) if selection $S3_x$ is applied. Also from figure 10, we can say that after selection $S3_x$, even with 3000 fb^{-1} integrated luminosity, the discovery prospects will be challenging if the neutral state mass is greater than 475 GeV.

In the 3SSL channel, exactly three same-sign leptons (eee or $\mu\mu\mu$ or $e\mu\mu$ or $ee\mu$) are required to pass the selections $S1$ and $S2$ (see table 3). These two selections are sufficient to suppress the backgrounds. Moreover, as the signal cross-section is small, implementing the $S3$ selection criterion reduces the signal cross-section significantly. Table 6 and table 7 gives the signal and background cross-section respectively after the selections ($S1$ and $S2$) for 3SSL channel at the 13 TeV LHC. It is clear from the table that selection $S2$ is sufficient

JHEP01(2019)080

$M_{\chi^{n\pm}}$ (GeV)	$\sigma(fb)\times$ BR	$S1$ (fb)	$S2$ (fb)
200,205,216,233,257	71.9	0.158	0.129
300,307,322,345,377	11.23	0.110	0.091
400,409,428,456,494	3.7	0.091	0.067
500,511,533,566,610	1.47	0.053	0.034
600,613,638,675,725	0.7	0.030	0.016
700,714,742,783,838	0.35	0.017	0.007
800,816,846,891,950	0.19	0.013	0.003

Table 6. Signal cross-sections after passing the various selection criteria in the 3SSL channel at the 13 TeV LHC for different masses of the quintuplet. Here n runs from 0 to 4 in a given quintuplet. We consider BR($\chi^{Q+1} \to l\nu\chi^{Q}$) = 0.22 where $l = e, \mu$ and BR($\chi^{Q+1} \to q\bar{q}\chi^{Q}$) = 0.67.

Process	Cross-section (fb)	$S1$ (fb)	$S2$ (fb)
$pp \to t\bar{t}h$	508.5	9.1×10^{-4}	0
$pp \to t\bar{t}Z$	920	3.6×10^{-4}	0
$pp \to t\bar{t}W$	600	2.9×10^{-4}	1.5×10^{-4}
$pp \to WWZ$	103	0	0
$pp \to WZZ$	66	1.5×10^{-3}	8.5×10^{-6}
$pp \to ZZZ$	13.3	1.5×10^{-4}	0
$pp \to t\bar{t}t\bar{t}$	15.33	0.91×10^{-4}	0
$pp \to t\bar{t}b\bar{b}$	2638	2.2×10^{-4}	0
Total	-	3×10^{-3}	1.55×10^{-4}

Table 7. Background cross-sections in the 3SSL channel after passing the selection criteria $S1$ (third column) and $S2$ (fourth column) at the 13 TeV LHC.

to make prediction for exclusion and discovery as the total background becomes sufficiently small with $t\bar{t}W$ being the dominant background. The results for the exclusion and discovery are calculated as before and shown in figure 11. A quintuplet with neutral state mass (M_{χ^0}) up to 800 GeV can be excluded with only 500 fb^{-1} luminosity. As the signal cross-section is small in 3SSL channel, we also plot the required luminosity to observe 10 signal events (red line in figure 11). A quintuplet with neutral state mass $M_{\chi^0} \leq 800$ GeV can be excluded with 800 fb^{-1} luminosity if at least 10 signal events are required. It might be also possible to discover a M_{χ^0} up to 750 GeV with 1000 fb^{-1} luminosity.

The 4SSL channel can provide a very clean signature as the background is almost nonexistent. The events are required to pass both $S1$ and $S2$, but the signal cross-section becomes quite small if we impose $S2$. For example, if the mass of the neutral state of the quintuplet is 300 GeV, the signal cross-section after passing $S2$ is only 0.003 fb. If the same selection criteria is applied, this channel has practically zero background, smaller by

JHEP01(2019)080

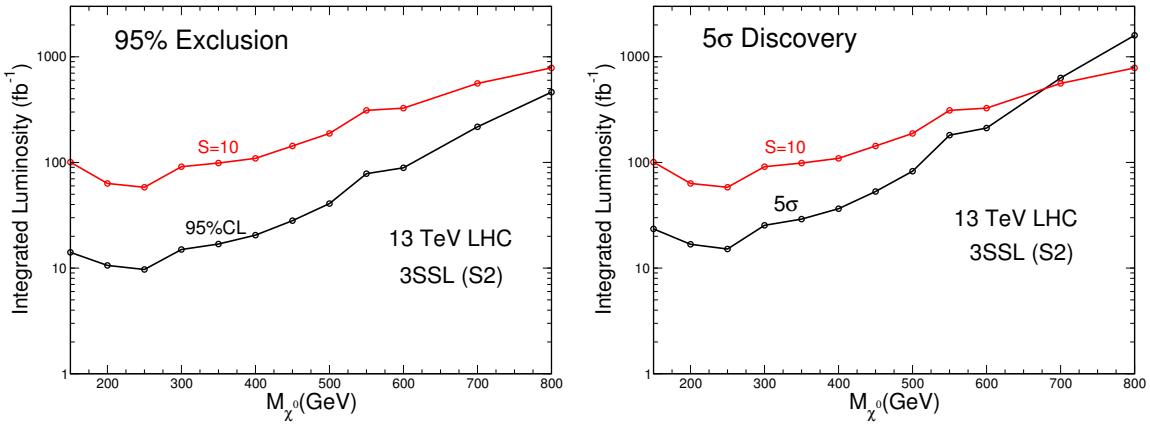

Figure 11. The left panel shows the required integrated luminosity at the 13 TeV LHC for 95% CL exclusion ($Z_{\rm exc} \geq 1.645$) in the 3SSL channel after imposing $S2$ selection criteria as a function of M_{χ^0}. The right panel portrays the same for 5σ discovery ($Z_{\rm dis} \geq 5$). Note that the results remain same for any uncertainty in the background in the range 0 to 50%. In both the panels (red lines), we also show the required integrated luminosity to observe 10 signal events in the 3SSL channel.

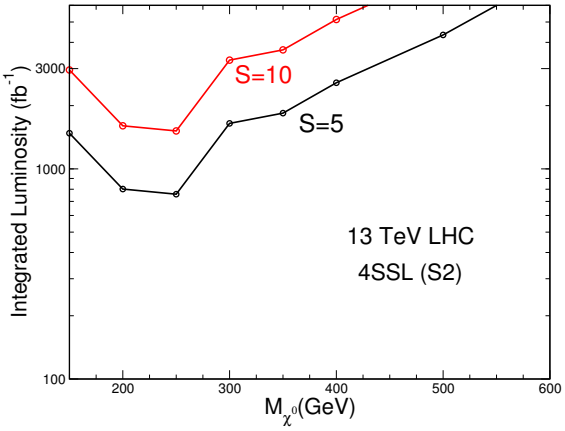

Figure 12. The black and red lines depict the required integrated luminosity at the 13 TeV LHC to observe at least 5 and 10 signal events respectively in the 4SSL channel after imposing the $S2$ selection criteria as a function of the neutral state mass (M_{χ^0}).

a factor of α compared to 3SSL channel. Hence, in figure 12, we only plot the required luminosity to observe 5 and 10 signal events as a function of the neutral state mass (M_{χ^0}) at 13 TeV if selection $S2$ is imposed. We find that for 300 GeV neutral state mass, the required luminosity will be greater than 3000 fb^{-1} in order to see 10 signal events.

5 Concluding remarks

In this paper, we consider the left-right symmetric model with a SU(2)$_R$ quintuplet fermion. The neutral state of this quintuplet, which is also the lightest, can be a viable dark matter candidate, while its charged fields can give rich collider signatures in the form of the multilepton final states. We study in detail the collider imprints of the same-sign multilepton

JHEP01(2019)080

final states in the context of the 13 TeV LHC. We consider the scenario where the quintuplet fermion possesses $(B-L) = 4$ charge, since it gives the most interesting collider signatures due to the presence of high charge-multiplicity particles producing lepton-rich final states.

These high charge-multiplicity particles can be pair produced through quark-antiquark initiated Drell-Yan processes or through photo production by photon-photon fusion process. Here, we show that the photon-photon fusion process contributes significantly in the total cross-section of the quintuplet fermions at the 13 TeV LHC. They can also have associated production into two quintuplet fermions of different charges through a W_R boson. But, the production cross-section of this channel would be negligibly small. Once produced, the quintuplet fermions decay into the next lightest member of that quintuplet and two leptons or two quarks through an off-shell W_R boson. This ultimately gives rise to final states comprising of a number of leptons, jets, and missing energy. Here, we study the same-sign multilepton signatures such as 2SSL, 3SSL, and 4SSL final states in the context of the LHC experiment at 13 TeV.

For our analysis, we consider several benchmark points with the neutral state mass (M_{χ^0}) of the quintuplet ranging from 200 GeV to 800 GeV. For the 2SSL case $M_{\chi^0} \leq 610$ GeV can be we can excluded at 95% confidence level for 3000 fb^{-1} luminosity. The discovery prospect at 5σ level, being much more challenging, has an upper limit of $M_{\chi^0} \leq 475$ GeV. As far as the 3SSL channel is concerned, it has a much lower background as compared to the 2SSL channel. This enhances both the exclusion and discovery potential in the 3SSL channel. The LHC at 13 TeV would be able to exclude a $M_{\chi^0} \leq 800$ GeV at 95% CL with an integrated luminosity of 500 fb^{-1}. Discovery at 5σ is achievable upto $M_{\chi^0} \leq 750$ GeV with 1000 fb^{-1} luminosity. The 4SSL is the cleanest channel with almost zero background, but at the same time it will have a very small signal cross-section which makes it extremely difficult to place a limit for exclusion or predict any discovery potential.

Overall, our study reflects that with the 13 TeV LHC, a 5σ discovery reach or a 95% CL exclusion limit on the $\text{SU}(2)_R$ quintuplet mass can be achieved by observing the same-sign multilepton signatures. We hope that the study performed in this paper will add to the long standing quest to search for new physics at LHC through the same-sign multilepton final states.

Acknowledgments

We thank Dr. Biplob Bhattacherjee for useful comments. S.K.A. acknowledges the support from the DST/INSPIRE Research Grant [IFA-PH-12], Department of Science and Technology, India and the Young Scientist Project [INSA/SP/YSP/144/2017/1578] from the Indian National Science Academy. K.G. acknowledges the support from the DST/INSPIRE Research Grant [DST/INSPIRE/04/2014/002158]. N.K. acknowledges the support from the Indo-French Center for Promotion of Advanced Research (CEFIPRA Project No. 5404-2). N.K. would like to thank Institute of Physics, Bhubaneswar for hospitality at the initial stage of the project. A.P. is supported by the SERB National Postdoctoral fellowship [PDF/2016/000202]. A.P. and N.K. thank the organizers of "Candles of Darkness" conference held at ICTS, Bangalore, India during June, 2017 for giving the opportunity to

JHEP01(2019)080

present the preliminary results of this work. N.K. also thanks the organizers of "SUSY17" for providing the opportunity to present and discuss the results of this paper.

References

[1] P. Ko and T. Nomura, $SU(2)_L \times SU(2)_R$ *minimal dark matter with* 2 *TeV* W', *Phys. Lett.* **B 753** (2016) 612 [arXiv:1510.07872] [INSPIRE].

[2] S.K. Agarwalla, K. Ghosh and A. Patra, *LHC diphoton excess in a left-right symmetric model with minimal dark matter*, arXiv:1607.03878 [INSPIRE].

[3] S. Kumar Agarwalla, K. Ghosh and A. Patra, *Sub-TeV quintuplet minimal dark matter with left-right symmetry*, *JHEP* **05** (2018) 123 [arXiv:1803.01670] [INSPIRE].

[4] M. Cirelli, N. Fornengo and A. Strumia, *Minimal dark matter*, *Nucl. Phys.* **B 753** (2006) 178 [hep-ph/0512090] [INSPIRE].

[5] J. Heeck and S. Patra, *Minimal left-right symmetric dark matter*, *Phys. Rev. Lett.* **115** (2015) 121804 [arXiv:1507.01584] [INSPIRE].

[6] C. Garcia-Cely and J. Heeck, *Phenomenology of left-right symmetric dark matter*, arXiv:1512.03332 [INSPIRE].

[7] N. Maru, N. Okada and S. Okada, *Fermionic minimal dark matter in* 5*D gauge-Higgs unification*, *Phys. Rev.* **D 96** (2017) 115023 [arXiv:1801.00686] [INSPIRE].

[8] B. Ostdiek, *Constraining the minimal dark matter fiveplet with LHC searches*, *Phys. Rev.* **D 92** (2015) 055008 [arXiv:1506.03445] [INSPIRE].

[9] K. Kumericki, I. Picek and B. Radovcic, *TeV-scale seesaw with quintuplet fermions*, *Phys. Rev.* **D 86** (2012) 013006 [arXiv:1204.6599] [INSPIRE].

[10] Y. Yu, C.-X. Yue and S. Yang, *Signatures of the quintuplet leptons at the LHC*, *Phys. Rev.* **D 91** (2015) 093003 [arXiv:1502.02801] [INSPIRE].

[11] R.N. Mohapatra and J.C. Pati, *Left-right gauge symmetry and an isoconjugate model of CP-violation*, *Phys. Rev.* **D 11** (1975) 566 [INSPIRE].

[12] G. Senjanović and R.N. Mohapatra, *Exact left-right symmetry and spontaneous violation of parity*, *Phys. Rev.* **D 12** (1975) 1502 [INSPIRE].

[13] M.A.B. Beg and H.S. Tsao, *Strong* P, T *noninvariances in a superweak theory*, *Phys. Rev. Lett.* **41** (1978) 278 [INSPIRE].

[14] R.N. Mohapatra and G. Senjanović, *Natural suppression of strong* P *and* T *noninvariance*, *Phys. Lett.* **B 79** (1978) 283 [INSPIRE].

[15] K.S. Babu and R.N. Mohapatra, *A solution to the strong CP problem without an axion*, *Phys. Rev.* **D 41** (1990) 1286 [INSPIRE].

[16] S.M. Barr, D. Chang and G. Senjanović, *Strong CP problem and parity*, *Phys. Rev. Lett.* **67** (1991) 2765 [INSPIRE].

JHEP01(2019)080

[17] R.N. Mohapatra and A. Rasin, *Simple supersymmetric solution to the strong CP problem*, *Phys. Rev. Lett.* **76** (1996) 3490 [hep-ph/9511391] [INSPIRE].

[18] R. Kuchimanchi, *Solution to the strong CP problem: supersymmetry with parity*, *Phys. Rev. Lett.* **76** (1996) 3486 [hep-ph/9511376] [INSPIRE].

[19] R.N. Mohapatra, A. Rasin and G. Senjanović, *P, C and strong CP in left-right supersymmetric models*, *Phys. Rev. Lett.* **79** (1997) 4744 [hep-ph/9707281] [INSPIRE].

[20] K.S. Babu, B. Dutta and R.N. Mohapatra, *Solving the strong CP and the SUSY phase problems with parity symmetry*, *Phys. Rev.* **D 65** (2002) 016005 [hep-ph/0107100] [INSPIRE].

[21] R. Kuchimanchi, *P/CP conserving CP/P violation solves strong CP problem*, *Phys. Rev.* **D 82** (2010) 116008 [arXiv:1009.5961] [INSPIRE].

[22] R.D. Peccei and H.R. Quinn, *CP conservation in the presence of instantons*, *Phys. Rev. Lett.* **38** (1977) 1440 [INSPIRE].

[23] B. Mukhopadhyaya and S. Mukhopadhyay, *Same-sign trileptons and four-leptons as signatures of new physics at the CERN Large Hadron Collider*, *Phys. Rev.* **D 82** (2010) 031501 [arXiv:1005.3051] [INSPIRE].

[24] S. Mukhopadhyay and B. Mukhopadhyaya, *Same-sign trileptons at the LHC: a window to lepton-number violating supersymmetry*, *Phys. Rev.* **D 84** (2011) 095001 [arXiv:1108.4921] [INSPIRE].

[25] G. Bambhaniya, J. Chakrabortty, S. Goswami and P. Konar, *Generation of neutrino mass from new physics at TeV scale and multilepton signatures at the LHC*, *Phys. Rev.* **D 88** (2013) 075006 [arXiv:1305.2795] [INSPIRE].

[26] E.J. Chun and P. Sharma, *Same-sign tetra-leptons from type II seesaw*, *JHEP* **08** (2012) 162 [arXiv:1206.6278] [INSPIRE].

[27] CMS collaboration, *Search for physics beyond the Standard Model in events with two leptons of same sign, missing transverse momentum and jets in proton-proton collisions at* $\sqrt{s} = 13$ *TeV*, *Eur. Phys. J.* **C 77** (2017) 578 [arXiv:1704.07323] [INSPIRE].

[28] ATLAS collaboration, *Inclusive search for same-sign dilepton signatures in pp collisions at* $\sqrt{s} = 7$ *TeV with the ATLAS detector*, *JHEP* **10** (2011) 107 [arXiv:1108.0366] [INSPIRE].

[29] ATLAS collaboration, *Search for squarks and gluinos in events with isolated leptons, jets and missing transverse momentum at* $\sqrt{s} = 8$ *TeV with the ATLAS detector*, *JHEP* **04** (2015) 116 [arXiv:1501.03555] [INSPIRE].

[30] ATLAS collaboration, *Search for squarks and gluinos in events with an isolated lepton, jets and missing transverse momentum at* $\sqrt{s} = 13$ *TeV with the ATLAS detector*, *Phys. Rev.* **D 96** (2017) 112010 [arXiv:1708.08232] [INSPIRE].

[31] ATLAS collaboration, *Search for new phenomena using the invariant mass distribution of same-flavour opposite-sign dilepton pairs in events with missing transverse momentum in* $\sqrt{s} = 13$ *TeV pp collisions with the ATLAS detector*, *Eur. Phys. J.* **C 78** (2018) 625 [arXiv:1805.11381] [INSPIRE].

[32] CMS collaboration, *Search for new physics in events with two soft oppositely charged leptons and missing transverse momentum in proton-proton collisions at* $\sqrt{s} = 13$ *TeV*, *Phys. Lett.* **B 782** (2018) 440 [arXiv:1801.01846] [INSPIRE].

JHEP01(2019)080

[33] P. Minkowski, $\mu \to e\gamma$ *at a rate of one out of* 10^9 *muon decays?*, *Phys. Lett.* **B 67** (1977) 421 [INSPIRE].

[34] T. Yanagida, *Horizontal gauge symmetry and masses of neutrinos*, *Conf. Proc.* **C 7902131** (1979) 95 [INSPIRE].

[35] O. Sawada and A. Sugamoto eds., *Proceedings: workshop on the unified theories and the baryon number in the universe*, Natl. Lab. High Energy Phys., Tsukuba, Japan (1979) [INSPIRE].

[36] M. Lévy, J.L. Basdevant, D. Speiser, J. Weyers, R. Gastmans and M. Jacob eds., *Quarks and leptons. Proceedings, summer institute, Cargèse, France,* 9–29 *July* 1979, *NATO Sci. Ser.* **B 61** (1980) 1 [INSPIRE].

[37] P. Van Nieuwenhuizen and D.Z. Freedman eds., *Supergravity. Proceedings, workshop at Stony Brook,* 27–29 *September* 1979, North-Holland, Amsterdam, The Netherlands (1979) [INSPIRE].

[38] R.N. Mohapatra and G. Senjanović, *Neutrino mass and spontaneous parity nonconservation*, *Phys. Rev. Lett.* **44** (1980) 912 [INSPIRE].

[39] D. Chang, R.N. Mohapatra and M.K. Parida, *Decoupling parity and* $\mathrm{SU}(2)_R$ *breaking scales: a new approach to left-right symmetric models*, *Phys. Rev. Lett.* **52** (1984) 1072 [INSPIRE].

[40] NNPDF collaboration, *Parton distributions for the LHC run II*, *JHEP* **04** (2015) 040 [arXiv:1410.8849] [INSPIRE].

[41] NNPDF collaboration, *Parton distributions with QED corrections*, *Nucl. Phys.* **B 877** (2013) 290 [arXiv:1308.0598] [INSPIRE].

[42] A.D. Martin, R.G. Roberts, W.J. Stirling and R.S. Thorne, *Parton distributions incorporating QED contributions*, *Eur. Phys. J.* **C 39** (2005) 155 [hep-ph/0411040] [INSPIRE].

[43] C. Schmidt, J. Pumplin, D. Stump and C.P. Yuan, *CT14QED parton distribution functions from isolated photon production in deep inelastic scattering*, *Phys. Rev.* **D 93** (2016) 114015 [arXiv:1509.02905] [INSPIRE].

[44] A. Alloul, N.D. Christensen, C. Degrande, C. Duhr and B. Fuks, *FeynRules* 2.0 — *a complete toolbox for tree-level phenomenology*, *Comput. Phys. Commun.* **185** (2014) 2250 [arXiv:1310.1921] [INSPIRE].

[45] N.D. Christensen and C. Duhr, *FeynRules — Feynman rules made easy*, *Comput. Phys. Commun.* **180** (2009) 1614 [arXiv:0806.4194] [INSPIRE].

[46] J. Alwall et al., *The automated computation of tree-level and next-to-leading order differential cross sections and their matching to parton shower simulations*, *JHEP* **07** (2014) 079 [arXiv:1405.0301] [INSPIRE].

[47] R.D. Ball et al., *Parton distributions with LHC data*, *Nucl. Phys.* **B 867** (2013) 244 [arXiv:1207.1303] [INSPIRE].

[48] J. Alwall, M. Herquet, F. Maltoni, O. Mattelaer and T. Stelzer, *MadGraph* 5*: going beyond*, *JHEP* **06** (2011) 128 [arXiv:1106.0522] [INSPIRE].

[49] T. Sjöstrand, S. Mrenna and P.Z. Skands, *PYTHIA* 6.4 *physics and manual*, *JHEP* **05** (2006) 026 [hep-ph/0603175] [INSPIRE].

JHEP01(2019)080

[50] DELPHES 3 collaboration, *DELPHES 3, a modular framework for fast simulation of a generic collider experiment*, *JHEP* **02** (2014) 057 [arXiv:1307.6346] [INSPIRE].

[51] CMS collaboration, *Study of vector boson scattering and search for new physics in events with two same-sign leptons and two jets*, *Phys. Rev. Lett.* **114** (2015) 051801 [arXiv:1410.6315] [INSPIRE].

[52] J.M. Campbell and R.K. Ellis, *An update on vector boson pair production at hadron colliders*, *Phys. Rev.* **D 60** (1999) 113006 [hep-ph/9905386] [INSPIRE].

[53] F. Campanario, V. Hankele, C. Oleari, S. Prestel and D. Zeppenfeld, *QCD corrections to charged triple vector boson production with leptonic decay*, *Phys. Rev.* **D 78** (2008) 094012 [arXiv:0809.0790] [INSPIRE].

[54] M.V. Garzelli, A. Kardos, C.G. Papadopoulos and Z. Trócsányi, $t\bar{t}W^{\pm}$ *and* $t\bar{t}Z$ *hadroproduction at NLO accuracy in QCD with parton shower and hadronization effects*, *JHEP* **11** (2012) 056 [arXiv:1208.2665] [INSPIRE].

[55] LHC Higgs Cross Section Working Group collaboration, *Handbook of LHC Higgs cross sections: 3. Higgs properties*, arXiv:1307.1347 [INSPIRE].

[56] Y.-B. Shen, R.-Y. Zhang, W.-G. Ma, X.-Z. Li, Y. Zhang and L. Guo, *NLO QCD + NLO EW corrections to WZZ productions with leptonic decays at the LHC*, *JHEP* **10** (2015) 186 [*Erratum ibid.* **10** (2016) 156] [arXiv:1507.03693] [INSPIRE].

[57] D.T. Nhung, L.D. Ninh and M.M. Weber, *NLO corrections to WWZ production at the LHC*, *JHEP* **12** (2013) 096 [arXiv:1307.7403] [INSPIRE].

[58] A. Bredenstein, A. Denner, S. Dittmaier and S. Pozzorini, *NLO QCD corrections to* $pp \to t\bar{t}b\bar{b} + X$ *at the LHC*, *Phys. Rev. Lett.* **103** (2009) 012002 [arXiv:0905.0110] [INSPIRE].

[59] G. Bevilacqua and M. Worek, *Constraining BSM physics at the LHC: four top final states with NLO accuracy in perturbative QCD*, *JHEP* **07** (2012) 111 [arXiv:1206.3064] [INSPIRE].

[60] G. Cowan, *Two developments in discovery tests: use of weighted Monte Carlo events and an improved measure of experimental sensitivity*, talk given during the meeting on Progress on Statistical Issues in Searches, http://www-conf.slac.stanford.edu/statisticalissues2012/talks/glen_cowan_slac_4jun12.pdf, SLAC, Menlo Park, CA, U.S.A. 4–6 June 2012.

[61] N. Kumar and S.P. Martin, *Vectorlike leptons at the Large Hadron Collider*, *Phys. Rev.* **D 92** (2015) 115018 [arXiv:1510.03456] [INSPIRE].

[62] V.E. Ozcan, S. Sultansoy and G. Unel, *Possible discovery channel for new charged leptons at the LHC*, *J. Phys.* **G 36** (2009) 095002 [*Erratum ibid.* **G 37** (2010) 059801] [arXiv:0903.3177] [INSPIRE].

JHEP01(2019)080